Simulation of Four Quadrant Operation & Speed Control of BLDC Motor on MATLAB / SIMULINK

Vinatha U, *Research Scholar*, Swetha Pola, *Asst. Software Engg.,* TCS, Dr K.P.Vittal, *Asst. Prof.,* MIEEE Dept. of Electrical & Electronics Engineering, National Inst. of Technology, Surathkal, India 575025
swetha.pola@tcs.com

Abstract-- **BLDC motors have been gaining attention from various Industrial and household appliance manufacturers, because of its high efficiency, high power density and low maintenance cost. After many research and developments in the fields of magnetic materials and power electronics, their applications to electric drives have increased to a significant extent. In this paper, the modeling of Brushless DC motor drive system along with control system for speed and current has been presented using MATLAB / SIMULINK. In order to evaluate the model, various cases of simulation studies are carried out. Test results thus obtained show that, the model performance is satisfactory.**

I. INTRODUCTION

Brushless DC motors have been used in various industrial and domestic applications. Due to overweighing merits of this motor, there is continuing trend to propose improved control schemes to enhance the performance of the motor.

For analysis of the BLDC motor drives system under various conditions, models such as d-q model and abc phase variable models have been developed [3,7].

Several simulation models were proposed [1]-[4] based on non-linear state-space equations. BLDC Motor considered in these models is star connected with neutral grounding, but several applications require isolated neutral [8]. Keeping merits of these developments in view, in this paper the motor is modeled as star connected with isolated neutral and the voltages supplied are line-line.

Modeling the complete control scheme is beneficial in carrying out the comprehensive simulation studies. Such comprehensive simulation studies are not reported. This paper deals with simulation models of PWM inverter and the controllers for the BLDC motor. The performance of this simulation is examined under no-load, variable load at variable speeds, blocked rotor and intermittent loads. In addition, four quadrant operation of BLDC motor is also carried out.

II. DESCRIPTION AND MODELING OF THE DRIVE SYSTEM

The complete drive system is shown in Fig. 1. It can be categorized into BLDC motor, Inverter, Current Controller, Speed Controller and Quad Determination Block for Four-Quadrant Operation. Each block is modeled separately and integrated together.

A. Modeling of BLDC motor

BLDC motor can be realized mathematically in two ways: abc phase variable model and d-q axis model. In a BLDC motor, the trapezoidal back EMF implies that the mutual inductance between stator and rotor is non-sinusoidal, thus transforming to d-q axis does not provide any particular advantage, and so abc phase variable model is preferred.

In the present model, the motor is assumed to be star connected with isolated neutral. Following assumptions are made in modeling the motor.

- The motor is not saturated.
- Stator resistances of all the windings are equal and self and mutual inductances are constant.
- Ideal power semiconductor devices.

The electrical and mechanical system is realized as:

$$\frac{di_a}{dt} = -\left(\frac{di_b}{dt} + \frac{di_c}{dt}\right) \tag{1}$$

$$\frac{di_b}{dt} = \frac{1}{3L_T}[V_{ca} + 2V_{bc} - 3Ri_b + (e_a + e_c - 2e_b)] \tag{2}$$

$$\frac{di_c}{dt} = \frac{1}{3L_T}[V_{ca} - V_{bc} - 3Ri_c + (e_a + e_b - 2e_c)] \tag{3}$$

$$E_k = \sum_k K_e \omega_m f_k(\theta_r) \tag{4}$$

$$T_e = \sum_k K_t i_k f_k(\theta_r) \tag{5}$$

$$T_e - T_L = J\frac{d\omega_m}{dt} + B\omega_m \tag{6}$$

where $k = a, b, c$

i_k is the phase current of k_{th} phase

e_k is the back-EMF of k_{th} phase

T_e is the electromagnetic torque

ω_m is the mechanical speed of the motor

J is rotor inertia.

B is damping constant.

R_s is the resistance of each phase of the motor

L_t is the inductance of the each phase of the motor

K_t is torque constant

K_e is back-EMF constant

p is the number of poles

$f_k(\theta_r)$ represents the back-EMF as a function of rotor position.

The above equations are sub divided into mechanical and electrical equations representing the BLDC system.

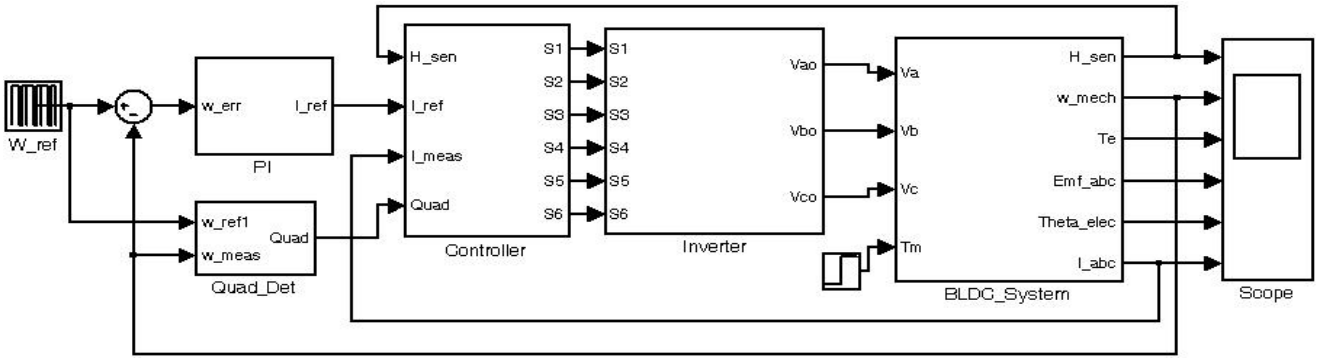

Fig. 1. SIMULINK MODEL OF BLDC DRIVE SYSTEM

The electrical system equation constitutes (1) to (5). Equation (1) to (3) is obtained by solving the loop equation (7) when an inverter is connected to a star load.

$$\begin{bmatrix} V_{an} \\ V_{bn} \\ V_{cn} \end{bmatrix} = R_s \begin{bmatrix} I_a \\ I_b \\ I_c \end{bmatrix} + (L_s + M) \begin{bmatrix} \frac{di_a}{dt} \\ \frac{di_b}{dt} \\ \frac{di_c}{dt} \end{bmatrix} + \begin{bmatrix} e_{an} \\ e_{bn} \\ e_{cn} \end{bmatrix} \qquad (7)$$

The back-EMF equations modeled [3] as a normalized function of rotor position is as shown in Table I.

TABLE I
BACK-EMF MODELED AS A FUNCTION OF ROTOR ANGLE

Theta_elec	$F_a(\theta_r)$	$F_b(\theta_r)$	$F_c(\theta_r)$
0^o-60^o	$\frac{6\theta_r}{\pi}-1$	+1	-1
60^o-120^o	+1	$3-\frac{6\theta_r}{\pi}$	-1
120^o-180^o	+1	-1	$\frac{6\theta_r}{\pi}-5$
180^o-240^o	$7-\frac{6\theta_r}{\pi}$	-1	+1
240^o-300^o	-1	$\frac{6\theta_r}{\pi}-9$	+1
300^o-360^o	-1	+1	$11-\frac{6\theta_r}{\pi}$

It may be observed that, the function shown in Table I are 120^o phase shifted. The modeling of the motor includes the realization of hall sensors as a function of rotor electrical angle which is listed in Table II.

B. Closed-Loop Controller

The BLDC motor is fed by a three phase MOSFET based inverter. The PWM gating signals for firing the power semiconductor devices in the inverter is injected from a hysteresis current controller [4] which is required to maintain the current constant within the 60^o interval of one electrical revolution of the rotor.

TABLE II
HALL SENSORS MODELED AS A FUNCTION OF ROTOR ANGLE

Theta_elec	**h_1 h_2 h_3**
0^o - 60^o	1 0 1
60^o - 120^o	0 0 1
120^o - 180^o	0 1 1
180^o - 240^o	0 1 0
240^o - 300^o	1 1 0
300^o - 360^o	1 0 0

It regulates the actual current within the hysteresis band around the reference currents. The reference currents are generated by a reference current generator depending upon the steady state operating mode. The reference currents are of quasi –square wave. They are developed in phase with the back-emf in motoring mode and out of phase in braking mode. The magnitude of the reference current is calculated from the reference torque. The reference torque is obtained by limiting the output of the PI controller. The PI controller processes on the speed error signal (i.e. the difference between the reference speed and actual speed) and outputs to the limiter to produce the reference torque. The actual speed is sensed back to the speed controller and processed on to minimize the error in tracking the reference speed. Thus, it is a closed loop control drive system.

C. Inverter Modeling

The inverter (Fig. 2.) supplies the input voltage for the three phases of the BLDC motor. It comprises of two power semiconductor devices on each phase leg. Appropriate pairs of FET's (S1 to S6) are driven based on the hall sensors input. Three phases are commutated for every 60^o.

As sensors are the direct feed back of the rotor position, synchronization between stator and rotor flux is achieved. The inverter is implemented using equations (8), (9) and (10).

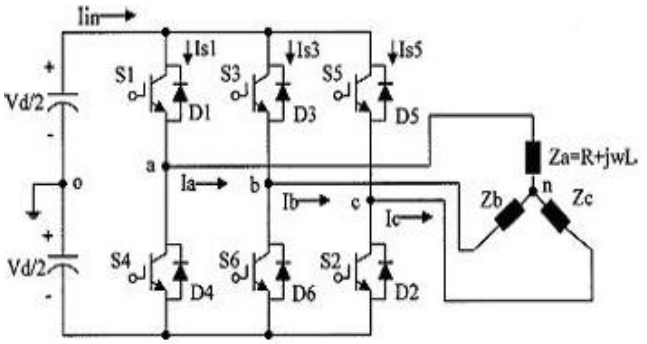

Fig. 2. Three Phase MOSFET-Based Inverter

$$V_{AN} = (S_1) * (\frac{V_d}{2}) - (S_4) * (\frac{V_d}{2}) - V_F \quad (8)$$

$$V_{BN} = (S_3) * (\frac{V_d}{2}) - (S_6) * (\frac{V_d}{2}) - V_F \quad (9)$$

$$V_{CN} = (S_5) * (\frac{V_d}{2}) - (S_2) * (\frac{V_d}{2}) - V_F \quad (10)$$

where V_{AN} , V_{BN} and V_{CN} are line-neutral voltages

V_d is the DC-link voltage.

V_F is the forward diode voltage drop.

D. Modeling of Hysteresis Controller

Hysteresis controller [4] limits the phase currents within the hysteresis band by switching ON/OFF the power devices. The switching pattern is given as:

If $i_a^{err} > UL$, S1 is on and S4 is off.

If $i_a^{err} < LL$, S1 is off and S4 is on.

If $i_b^{err} > UL$, S3 is on and S6 is off.

If $i_b^{err} < LL$, S3 is off and S6 is on.

If $i_c^{err} > UL$, S5 is on and S2 is off.

If $i_c^{err} < LL$, S5 is off and S2 is on.

where $i_k^{err} = i_k^{ref} - i_k^{meas}$ and UL, LL are the upper and lower limits of hysteresis band. Thus, by regulating the current desired quasi-square waveforms can be obtained.

E. Modeling of Reference Current Generator

The desired reference currents are injected into the hysteresis controller. The magnitude of the reference current is determined from the reference torque and back-emf constant. The incoming or outgoing direction of the current is determined from hall sensors output and the operating mode. The reference currents for four steady state operations are modeled as shown in Table III (Forward motoring and reverse braking) and Table IV (Reverse motoring and forward braking:

TABLE III
REFERENCE CURRENTS FOR FORWARD MOTORING AND REVERSE BRAKING

h_1 h_2 h_3	I_a^{ref}	I_b^{ref}	I_c^{ref}
1 0 1	0	I^*	$-I^*$
0 0 1	I^*	0	$-I^*$
0 1 1	I^*	$-I^*$	0
0 1 0	0	$-I^*$	I^*
1 1 0	$-I^*$	0	I^*
1 0 0	$-I^*$	I^*	0

TABLE IV
REFERENCE CURRENTS FOR REVERSE MOTORING AND FORWARD BRAKING

h_1 h_2 h_3	I_a^{ref}	I_b^{ref}	I_c^{ref}
1 0 1	0	$-I^*$	I^*
0 0 1	$-I^*$	0	I^*
0 1 1	$-I^*$	I^*	0
0 1 0	0	I^*	$-I^*$
1 1 0	I^*	0	$-I^*$
1 0 0	I^*	$-I^*$	0

F. Modeling of Speed Controller

Conventional PI controller is used as a speed controller for recovering the actual motor speed to the reference. The reference and the measured speed are the input signals to the PI controller. The K_P and K_I values of the controller are determined by trial and error method for each set speed. The controller output is limited to give the reference torque.

G. Modeling of Quadrant Determination subsystem

The set speed and the actual speed determine the operating mode of the motor. Based on the quadrant in which the motor operates, the required reference currents are generated.

III. SIMULATION RESULTS AND DISCUSSION

Since the model equations are of non-linear in nature, they are solved by Runge-Kutta numerical technique simulated using MATLAB/SIMULINK. The performance of the developed BLDC system model is examined using motor parameters as listed in Table V [5].

TABLE V
MOTOR SPECIFICATIONS

V_{dc},(v)	380	K_b(v/rad/sec)	0.13658
P	4	J(Kg-m^2)	0.0022
R_s (Ω)	0.7	ω_{rated} (rpm)	4000
L_t (H)	0.00521	T_{max}, (N-m)	2.73

Under following conditions the motor performance has been simulated and analyzed.

- Starting and No-load dynamics are discussed.

- Comparative study of motor response at different speeds when subjected to sudden load.
- Comparative study for different loads when applied suddenly at a particular set speed.
- Dynamics of the motor under blocked rotor conditions.
- For intermittent loads.
- Four - Quadrant operation of the BLDC motor.

A. Starting and No-Load Conditions

The starting dynamics of the motor is shown in Fig. 3. The reference speed is set at 2000 rpm. The starting current is limited to 20A by the controller. An electro-magnetic torque Te of 2.73 N-m is developed to start the motor from standstill. With the help of PI controller the actual speed is maintained at set value. As soon as the motor reaches the steady state speed at 0.172s, the starting current decreases to no-load current of 0.6A, Te decreases to 0.1 N-m and the trapezoidal back-emf settles at 28.62 V.

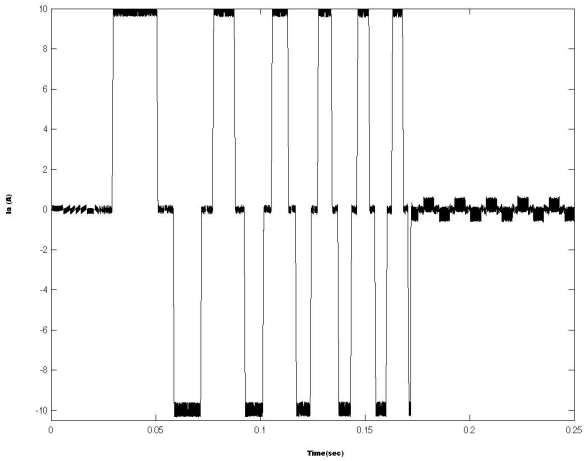

Fig. 3. Phase A Current at Starting and No-Load Conditions

B. Under Load Conditions

When a load is suddenly applied at 0.5s, there is a dip in the speed, but the controller recovers the speed to set value and thereby is no appreciable change in back-emf voltage. The current increases to 7.5 A to meet extra load with an increase in Te to 2.05 N-m as shown in Fig. 4. Once the load is removed all the parameters returns to no-load condition state. The Fig. 4 shows the efficiency of the current controller in achieving the rectangular load current.

C. Loading at Various Speeds

Under loaded conditions, at different speeds, motor dynamic behavior is analyzed. As the speed increases, time required to reach the steady state speed increases. Table VI shows the rise time and PI controller values.

Fig. 5. shows the torque-time characteristics for different speeds.

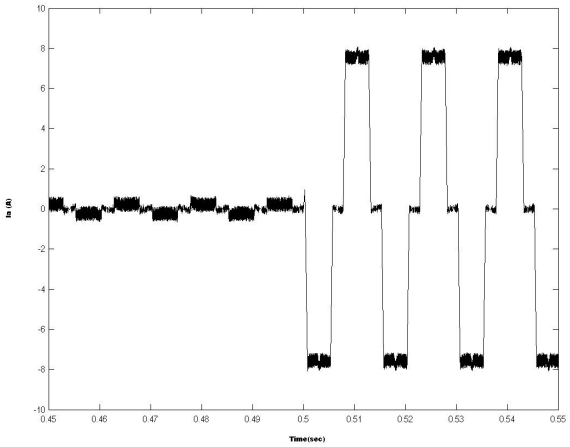

Fig. 4. Phase A Current under Load Conditions.

TABLE VI
K_P AND K_I VALUES FOR VARIOUS SPEEDS

W_{ref}	T_{rise}(sec)	K_p	K_i
2000	0.673	3.3	0.121
3000	1.06	21	0.789
4000	1.503	26	0.84

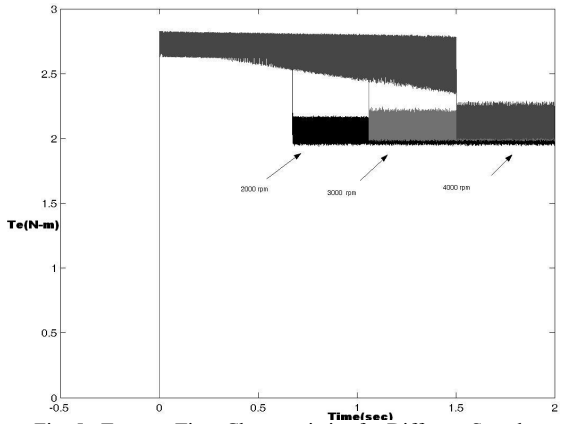

Fig. 5. Torque -Time Characteristics for Different Speeds.

D. Performance Under Loaded Condition

With reference speed set to 2000 rpm, motor is subjected to various loads.

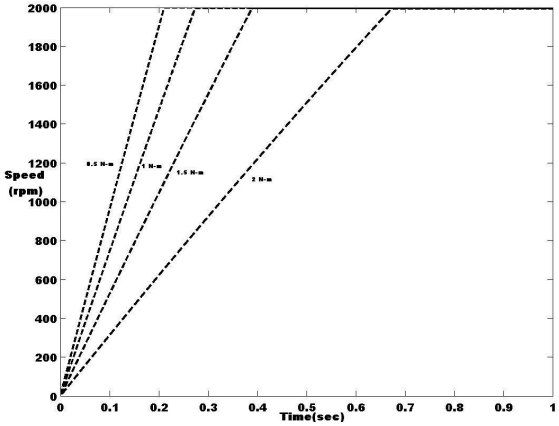

Fig. 6. Speed -Time Characteristics for Various Loads.

Fig.6 shows the speed - time characteristics for various

loads. The time taken to reach the set speed increases with the increment in load to be met. This can be observed in the Table VII.

TABLE VII
RISE TIME FOR DIFFERENT LOADS AT PARTICULAR REFERENCE SPEED

TL (N-m)	Rise Time (sec)
0.5	0.212
1	0.275
1.5	0.39
2	0.675

The realistic performance of the model is evident, as time taken time take to meet the maximum load is more when compared to that of minimum load. The torque characteristics for each load are shown in Fig. 7.

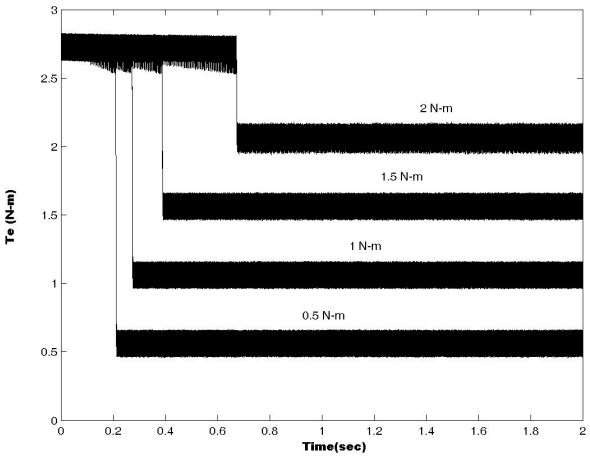

Fig. 7. Torque -Time Characteristics for Various Loads.

E. Under Blocked Rotor Conditions

Motor is loaded with the higher load torque than that of max. permissible torque. The moment the motor is loaded with higher Tl, the speed starts approaching to zero, also with back-emf developed tending to zero, as shown in Fig. 8.

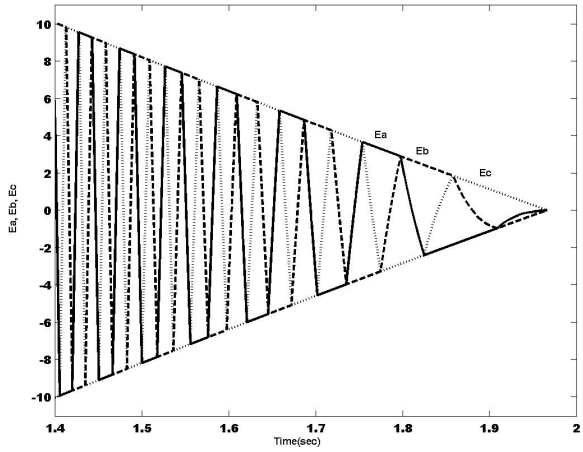

Fig. 8. Back-EMF Waveforms Under Blocked Rotor Conditions

The rotor decelerates to zero and is completely blocked at t=1.96s after applying a sudden load at 0.5s.

F. For Intermittent Loads

The motor drive system model also meets the intermittent loads. The motor speed performance at intermittent loads is shown in Fig. 9. It can be seen that the speed controller is capable of tracking the changes in the reference speed efficiently.

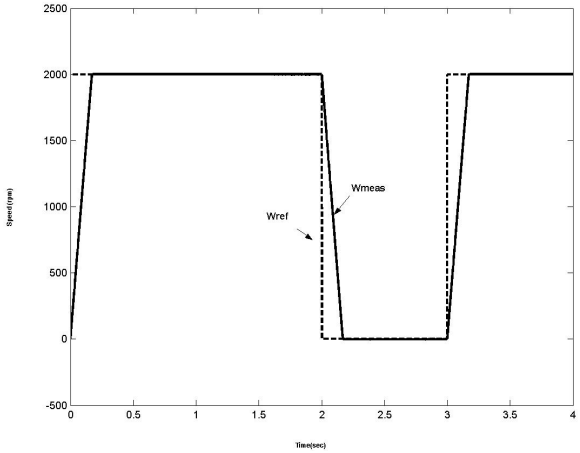

Fig. 9. Speed Profile for Intermittent Loads.

G. Four-Quadrant Operation

The motor is operated in four steady state operating modes of torque-speed plane. At initial conditions, the motor is operated in (Quad-I) Forward motoring mode. When a speed reversal command is issued, the motor undergoes braking operation in forward direction, with speed tending to zero and starts rotating in reverse direction as soon as the speed is zero.

The variation of rotor position when the motor is changing from forward braking mode to reverse motoring mode is shown in Fig. 10.

When a speed reversal command is issued again, the motor undergoes reverse braking and operates in Forward Motoring mode. In other words, motor rotates in forward direction. The rotor position varies as shown Fig. 11.

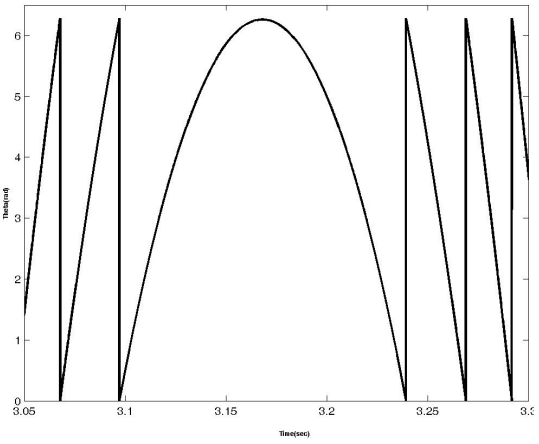

Fig. 10. Variation of Rotor Angle during Forward Braking to Reverse Motoring

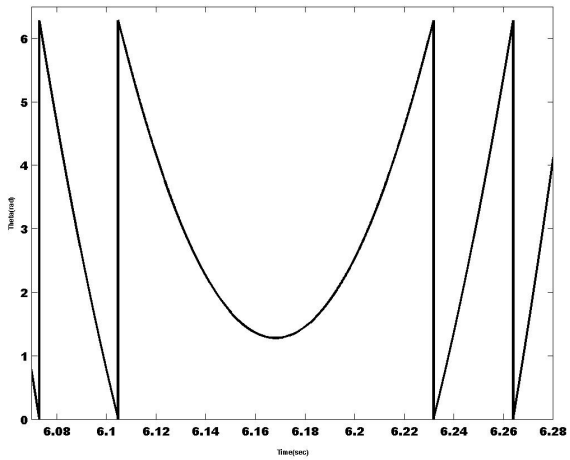

Fig. 11. Variation of Rotor Angle during Reverse Braking to Forward Motoring.

In the motoring mode, the back-emf magnitude increases until the steady state is reached and in braking mode back-emf starts decreasing towards zero. The Fig. 12 shows the change over of back–emf from braking mode to motoring mode. In the motoring mode, the corresponding back-emf and phase current is in phase. In braking mode [6], the back-EMF and phase current are out of phase as shown in the Fig. 12.

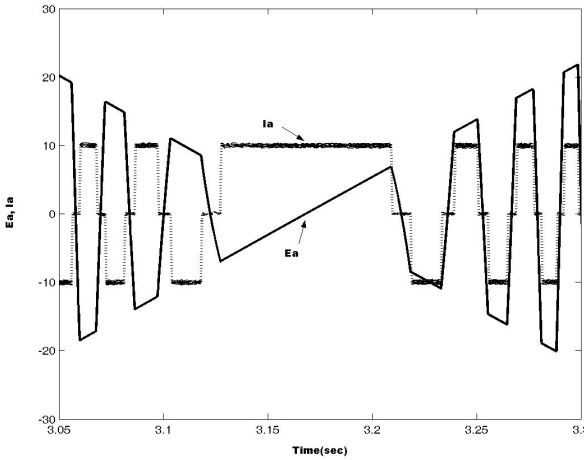

Fig. 12. Back-EMF and Current waveforms During Change Over from Braking Operation to Motoring Operation.

The traverse path of the operating point under four quadrant operation commands are depicted in Torque – Speed characteristics, as shown in the Fig. 13. In the Fig. 13, arrows indicate the traversal of speed-torque curve from first quadrant (Forward motoring) to third quadrant (Reverse Motoring) via second quadrant (Forward Braking) in four-quadrants.

IV. Conclusions

The modeling procedure presented in this paper helps in simulation of various operating conditions of BLDC drive system. The performance evaluation results show that, such a modeling is very useful in studying the drive system before taking up the dedicated controller design, accounting the relevant dynamic parameters of the motor.

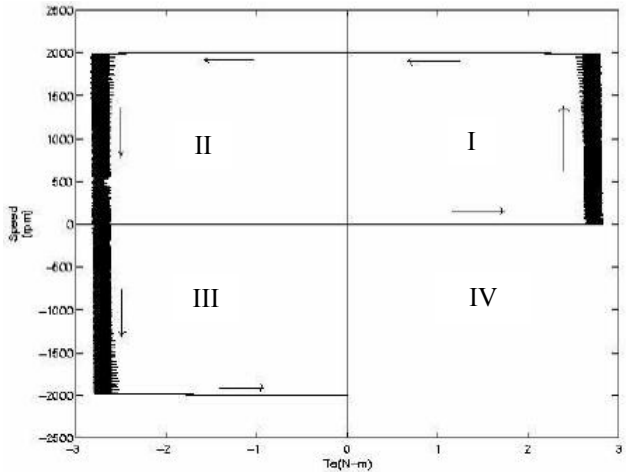

Fig. 13. Speed-Torque Characteristics

V. References

[1] P.Pillay and R.Krishnan, "Modeling, simulation and analysis of permanent-magnet motor drives, part-II: the brushless DC motor drives," *IEEE Trans. on Industry Applications*, vol. 25, pp.274-279, March/April 1989.

[2] S.K.Safi, P.P.Acarnley and A. G. Jack. "Analysis and simulation of the high-speed torque performance of brushless DC motor drives," *Proc. Of IEE*, vol 142, no.3, p.p.191-200, May 1995.

[3] Krishnan R motor "Drives Modeling, Analysis and Control", Prentice Hall of India, First Edn, 2002, Chapter 9, pp 513-615..

[4] Byoung-Kuk Lee and Mehrdad Ehsani, "Advanced Simulation Model for Brushless DC Motor Drives", Electric Power Component And Systems, 31:841-868, 2003.

[5] Dr.B.Singh, Prof B P Singh and C. L. Putta Swamy,"Modelling of Variable Structure Controlled Permanent Magnet Brushless dc Motor", *IE(I)*-Journal-EL, Vol 75, Febraury 1995.

[6] Gopal K Dubey "Fundamentals of Electrical Drives", Narosa Publishing House, New Delhi, Second Edn, 2001, Chapter 7, pp271-277.

[7] Bimal K Bose, "Modern Power Electronics and AC Drives", Pearson Education Publications, New Delhi, 2002, Chapter 9, pp483 - 495.

[8] Tae-Hyung Kim et al, IEEE publication no. 0-7803-7768-0/03.